# Scheduling and Power Control for V2V Broadcast Communications with Adjacent Channel Interference

Anver Hisham, Erik G. Ström, Fredrik Brännström, and Li Yan
Department of Electrical Engineering, Chalmers University of Technology, Gothenburg, Sweden
{anver, erik.strom, fredrik.brannstrom, lyaa}@chalmers.se

***Abstract*—This paper investigates how to mitigate the impact of adjacent channel interference (ACI) on vehicle-to-vehicle (V2V) broadcast communication by scheduling and power control. The optimal joint scheduling and power control problem, with the objective to maximize the number of connected vehicles, is formulated as a mixed integer programming problem with a linear objective and a quadratic constraint. From the joint formulation, we derive (a) the optimal scheduling problem for fixed transmit powers as a Boolean linear programming problem and (b) the optimal power control problem for a fixed schedule as a mixed integer linear programming problem. Near-optimal schedules and power values can, for smaller instances of the problem, be computed by solving first (a) and then (b). To handle larger instances of the problem, we propose heuristic scheduling and power control algorithms with reduced computational complexity. Simulation results indicate that the heuristic scheduling algorithm yields significant performance improvements compared to the baseline block-interleaver scheduler and that performance is further improved by the heuristic power control algorithm. Moreover, the heuristic algorithms perform close to the near-optimal scheme for small instances of the problem.**

## I. Introduction

### A. Motivation

Recently, vehicle-to-vehicle (V2V) communication have captured great attention due to its potential to improve traffic safety, effective driving assistance and intelligent transport systems. Typically, these types of applications have strict requirements on latency and reliability.

V2V networks have three novel features compared to conventional cellular communication. First, V2V networks generally rely on broadcast protocols to disseminate safety-related messages. Second, V2V communications often come with a stringent requirement on reliability, which can be achieved if the signal to interference and noise ratio (SINR) exceeds a certain threshold [1]. Third, low latency is an important requirement in V2V communication, which restricts the possibilities for retransmissions. Moreover, retransmission is cumbersome in a broadcast communication scenario. The determining factor for reliability in typical cellular communication is co-channel interference (CCI), which is crosstalk from two different transmitters using the same time-frequency slot. However, we can remove CCI (and thereby increase reliability) by allocating non-overlapping time-frequency resources to different vehicular user equipments (VUEs) for their transmissions [2].

The research was, in part, funded by the Swedish Governmental Agency for Innovation Systems (VINNOVA), FFI - Strategic Vehicle Research and Innovation, under Grant No. 2014-01387. This work has, in part, been performed in the framework of the H2020 project 5GCAR co-funded by the EU. The authors would like to acknowledge the contributions of their colleagues. The views expressed are those of the authors and do not necessarily represent the project. The consortium is not liable for any use that may be made of any of the information contained therein.

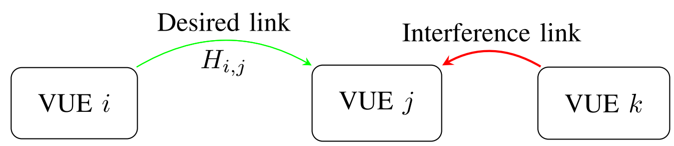


Fig. 1: System model

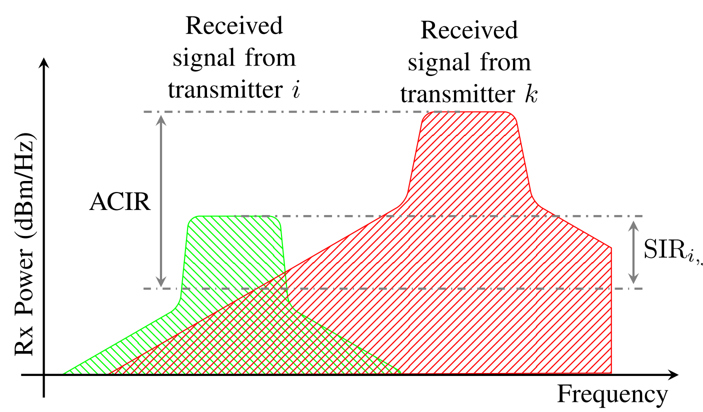


Fig. 2: Received power spectral density at receiving VUE $j$.

However, if two transmitters simultaneously operate on two non-overlapping frequency bands close to each other in the frequency domain, power from one transmitter will spill over into the frequency band of the other transmitter. This interference is termed adjacent channel interference (ACI) [3]. The ACI is mainly due to the nonlinearities in the power amplifier in the transmitter, which causes the transmitted spectrum to spread beyond what was intended. An example of ACI is illustrated in Fig. 1 and Fig. 2, where the receiver $j$ is decoding signals from transmitter $i$. Although transmitter $k$ is using a different frequency band, the signal to interference ratio $\mathrm{SIR}_{i,j}$, of receiver $j$ while decoding the signal from transmitter $i$ is limited by ACI from transmitter $k$. A parameter named adjacent channel interference ratio (ACIR) is widely used to measure the ACI [4, section 17.9]. As illustrated in Fig. 2, ACIR is defined as the ratio between the average in-band received power from transmitter $k$ to the average received out of band power from transmitter $k$'s signal in the frequency band allocated for transmitter $i$.

When the available time-frequency resources are sufficiently large, the VUEs can be allocated non-overlapping frequency bands in each time slot, thereby avoiding CCI. However, as already mentioned, the communication link performance is majorly limited by ACI in this scenario. Since the objective of this paper is to study the impact of ACI for V2V broadcast communication, we will limit the scope to the case when VUEs are allocated with non-overlapping time-frequency resources.

### B. State of the Art

In a typical cellular scenario, where each base station (BS) reuses the frequency spectrum, CCI would dominate over ACI. Since ACI is insignificant in the presence of CCI, most of the existing literature consider approaches to mitigate CCI alone [5]–[7]. However, in the absence of CCI, communication performance is majorly limited by ACI. Extensive studies have been done to measure the impact ACI when different communication technologies coexist in adjacent frequency bands [8]–[11]. Also, the impact of ACI on 802.11b/g/n/ac was broadly studied [12]–[14]. However, little attention have been made to study the effect of ACI within a V2V broadcast communication scenario in the absence of CCI. To further understand the impact of ACI in V2V broadcast communication in the absence of CCI, readers are directed to our previous work [15].

### C. Contributions

Our goal is to find scheduling and power control algorithms to maximize the number of connected vehicles in a V2V all-to-all broadcast communication scenario. We make the following contributions to achieve this goal:

1) The performance of V2V broadcast communication in the presence of ACI is evaluated.
2) We formulate the joint scheduling and power control problem to maximize the number of successful links as a mixed integer quadratically constrained programming (MIQCP) problem. From this, we derive the scheduling problem (for fixed transmit powers) as a boolean linear programming (BLP) problem and the power control problem (for a fixed schedule) as a mixed integer linear programming (MILP) problem. For small instances of the problem, we compute a near-optimal solution for scheduling by solving the BLP problem fomulation and then compute a near-optimal power values by solving the MILP problem fomulation.
3) Due to the NP hardness of the above problem formulation for scheduling, we suggest a block interleaver scheduler (BIS), which requires only the position indices of the VUEs.
4) We also propose a heuristic scheduling algorithm with polynomial time complexity. The simulation results show the promising performance of the heuristic algorithm, compared to the BIS and near-optimal scheduler.
5) Due to the NP hardness of the optimal power control problem, we propose a heuristic power control algorithm as an extension of our previous work in [15]. The simulation results show that the proposed algorithm further improves the performance compared to equal power.

## II. Preliminaries

### A. Notation

We use the following notation throughout the paper. Sets are denoted by calligraphic letters, e.g., $\mathcal{X}$, with $|\mathcal{X}|$ denoting its cardinality, and $\emptyset$ indicate an empty set. Lowercase and uppercase letters, e.g., $x$ and $X$, represent scalars. Lowercase boldface letters, e.g., $\mathbf{x}$, represent a vector where $x_i$ is the $i$th element and $|\mathbf{x}|$ is its dimensionality. The uppercase boldface letters, e.g., $\mathbf{X}$, denote matrices where $X_{i,j}$ indicates the $(i,j)^{\mathrm{th}}$ element. The notations $\lceil\cdot\rceil$, and $\lfloor\cdot\rfloor$, $\lfloor\cdot\rceil$ represents ceil, floor, and round operations, respectively.

### B. Assumptions

We have the following assumptions:

1) There are $N$ VUEs in the network, and each VUE wants to broadcast a safety message to all other VUEs within a specified time duration.
2) The total bandwidth for transmission is divided into $F$ frequency slots and the total time duration into $T$ timeslots. A time-frequency slot is also called a resource block (RB) [16, section 6.2.3]. We assume that a VUE can transmit its packet using a single RB.
3) A VUE's broadcast message can be received in an RB with the required error probability, if and only if the average received SINR is equal or greater than a threshold $\gamma^{\mathrm{T}}$. This assumption is valid, since in [1, Lemma 1], Sun et al. prove that achieving an SINR above a certain threshold ensures the required error probability.
4) Maximum total transmit power of a VUE is $P^{\max}$.
5) A centralized controller exists, which schedules all VUEs on $F \times T$ frequency-time slots and allocates powers to all VUEs. This centralized controller has access to the slowly varying channel state information (CSI) between all pairs of VUEs. Either a base station (BS) or a VUE can act as a centralized controller.
6) Each RB is scheduled to at most one VUE in order to avoid CCI.
7) A VUE is scheduled to at most one RB per timeslot, since scheduling in multiple RBs within the same timeslot would reduce the VUE's maximum transmit power per RB. However, a VUE can be scheduled on multiple RBs in different timeslots.

TABLE I: Key Mathematical Symbols

| Symbol | Definition |
|---|---|
| $N$ | Number of VUEs |
| $F$ | Number of frequency slots |
| $T$ | Number of timeslots |
| $P_{i,t}$ | Transmit power of VUE $i$ on an RB in timeslot $t$ |
| $P^{\max}$ | Maximum transmit power of a VUE |
| $H_{i,j}$ | Average channel power gain from VUE $i$ to VUE $j$ |
| $A_{f',f}$ | ACI from frequency slot $f'$ to frequency slot $f$ |
| $X_{i,f,t}$ | Indicate if VUE $i$ is scheduled to transmit in RB $(f,t)$ |
| $Y_{j,f,t}$ | Indicate if VUE $j$ receives packet successfully in RB $(f,t)$ |
| $\Upsilon_{i,j,t}$ | SINR of the packet from VUE $i$ to VUE $j$ in timeslot $t$ |
| $\Gamma_{j,f,t}$ | SINR of the packet received by VUE $j$ in RB $(f,t)$ |
| $\gamma^{\mathrm{T}}$ | SINR threshold to declare a link as successful |
| $\sigma^2$ | Noise variance in an RB |

### C. ACIR Model

ACI caused by a transmitter depends mainly upon the power amplifier and the transmission scheme used in the communication. In Fig. 3, the spectrum for a typical single carrier frequency division multiple access (SCFDMA) signal with a power amplifier of 1% clipping threshold is shown in blue color [17]. The red-colored step curve in the same figure shows the SCFDMA ACI averaged over each frequency slot. However, since the ACI is heavily dependent upon the power amplifier and the transmission scheme used in the communication, we will use the ACI mask specified by 3GPP [18] for the simulation purposes in this paper. Simulation results for the SCFDMA ACI model is available in the report [19], but is not presented here due to lack of space. We have observed by extensive simulations that, independent of the ACIR model, ACI plays a crucial role since it is higher than the noise floor for a typical communication link between neighbouring VUEs. Furthermore, whenever a transmitter is far away from the receiver and the interferers are close-by, ACI becomes a significant factor deciding received SINR. Indeed, the simulation results in the report [19] show that the order of performance for the algorithms is the same as the one presented in Section VI below, regardless of the ACIR model.

Let $\mathbf{A} \in \mathbb{R}^{F\times F}$ be the element-wise inverse ACIR matrix, i.e., $A_{f',f}$ is the ratio between the received power on the frequency slot $f$ and the received power on the frequency slot $f'$, when a transmitter sends a packet on frequency slot $f'$. Observe that $\mathbf{A}$ is a Toeplitz matrix. The mask specified by 3GPP [18] is as follows,

$$A_{f',f} = \begin{cases} 1, & f' = f \\ 10^{-3}, & 1 \le |f'-f| \le 4 \\ 10^{-4.5}, & \text{otherwise} \end{cases} \tag{1}$$

The scenario $f' = f$ in the above equation implies that VUEs are allocated within the same RB, in which case the interference would be CCI instead of ACI. In our study, this scenario never happens, due to our assumption 6) that no RB is scheduled to more than one VUE. The ACI, resulting from the 3GPP mask and from using SCFDMA are depicted in Fig. 3.

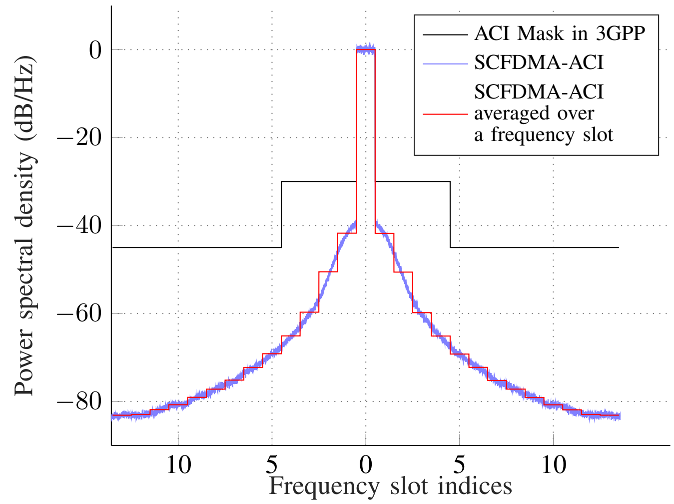


Fig. 3: Inverse ACIR model

## III. Joint Scheduling and Power Control

### A. Constraints Formulations

Let $H_{i,j}$ be the average channel power gain from VUE $i$ to VUE $j$. Hence, $H_{i,j}$ takes into account pathloss and large-scale fading between VUE $i$ and VUE $j$.

Let $\mathbf{X} \in \{0,1\}^{N\times F\times T}$ be the scheduling matrix defined as follows,

$$X_{i,f,t} \triangleq \begin{cases} 1, & \text{if VUE } i \text{ is scheduled in RB } (f,t) \\ 0, & \text{otherwise} \end{cases} \tag{2}$$

In order to ensure our assumption 6), i.e., an RB is scheduled to at most one VUE, $\mathbf{X}$ must satisfy the following condition,

$$\sum_{i=1}^{N} X_{i,f,t} \le 1 \quad \forall f,\, t \tag{3}$$

Similarly, to ensure our assumption 7), i.e., a VUE is scheduled to at most one RB in a timeslot,

$$\sum_{f=1}^{F} X_{i,f,t} \le 1 \quad \forall i,\, t \tag{4}$$

Formulating the scheduling problem to maximize the number of successful links in terms of the received SINR for VUE $j$ on RB $(f,t)$ will allow us to state the problem as an MIQCP problem. This is done with the support of our assumption 6) and 7) (i.e., constraints (3) and (4)). In contrast, as shown in Appendix A, a formulation using the SINR for specific transmitter-receiver pairs results in a problem that is harder to solve.

Let us define $\mathbf{\Gamma} \in \{0,1\}^{N\times F\times T}$ with $\Gamma_{j,f,t}$ as the received SINR of VUE $j$ in RB $(f,t)$. Note that the total signal power $S_{j,f,t}$ and interference power $I_{j,f,t}$ received by VUE $j$ in RB $(f,t)$ can be computed as follows,

$$S_{j,f,t} = \sum_{\substack{i=1 \\ i \neq j}}^{N} X_{i,f,t} P_{i,t} H_{i,j} \ , \tag{5}$$

$$I_{j,f,t} = \sum_{\substack{f'=1 \\ f' \neq f}}^{F} \sum_{k=1}^{N} A_{f',f} X_{k,f',t} P_{k,t} H_{k,j} \ , \tag{6}$$

where $\mathbf{P} \in \mathbb{R}^{N \times T}$ with $P_{i,t}$ being the transmit power of VUE $i$, if scheduled in timeslot $t$. The value of $P_{i,t}$ is constrained by maximum transmit power $P^{\max}$, i.e.,

$$0 \leq P_{i,t} \leq P^{\max} \qquad \forall\, i, t \tag{7}$$

Following (5) and (6), we can compute $\Gamma_{j,f,t}$ as follows,

$$\Gamma_{j,f,t} = \frac{S_{j,f,t}}{\sigma^2 + I_{j,f,t}}, \tag{8}$$

where $\sigma^2$ is the noise variance.

For successful links, $\Gamma_{j,f,t} \geq \gamma^{\mathrm{T}}$, i.e.,

$$S_{j,f,t} - \gamma^{\mathrm{T}} I_{j,f,t} \geq \gamma^{\mathrm{T}} \sigma^2. \tag{9}$$

However, it might not be possible to fulfill this condition for all receivers $j$ in all RBs $(f, t)$. To select which combinations of $j$, $f$, and $t$ to enforce this condition, we introduce the matrix $\mathbf{Y} \in \{0, 1\}^{N \times F \times T}$, where

$$Y_{j,f,t} \triangleq \begin{cases} 1, & \text{if (9) is enforced} \\ 0, & \text{otherwise} \end{cases} \tag{10}$$

We can combine (9) and (10) into a single constraint as

$$S_{j,f,t} - \gamma^{\mathrm{T}} I_{j,f,t} \geq \gamma^{\mathrm{T}} \sigma^2 - \eta(1 - Y_{j,f,t}) \qquad \forall j, f, t \tag{11}$$

where $\eta$ is a sufficiently large number to make (11) hold whenever $Y_{j,f,t} = 0$, regardless of the schedule and power allocation. It is not hard to show that $\eta = \gamma^{\mathrm{T}}(NP^{\max} + \sigma^2)$ is sufficient.

### B. Problem Formulation

We define a link as a transmitter-receiver pair $(i, j)$, and we say that the link $(i, j)$ is successful if at least one transmission from VUE $i$ to VUE $j$ is successful during the scheduling interval, i.e., that the SINR condition (9) is satisfied for at least one RB $(f, t)$ where $f \in \{1, 2, \ldots, F\}$ and $t \in \{1, 2, \ldots, T\}$. We introduce the matrix $\mathbf{Z} \in \{0, 1\}^{N \times N}$, where, for all $i, j$,

$$Z_{i,j} \triangleq \min\{1, \sum_{t=1}^{T} \sum_{f=1}^{F} X_{i,f,t} Y_{j,f,t}\} \tag{12}$$

$$= \begin{cases} 1, & \text{link } (i,j) \text{ is successful} \\ 0, & \text{otherwise} \end{cases} \tag{13}$$

We note that the minimum in (12) is required to not count successful links between VUE $i$ and VUE $j$ more than once.

The overall goal is to maximize the number of connected VUE pairs, i.e., to maximize the objective function

$$J(\mathbf{X}, \mathbf{Y}, \mathbf{P}) \triangleq \sum_{i=1}^{N} \sum_{\substack{j=1 \\ j \neq i}}^{N} Z_{i,j} \tag{14}$$

subject to the constraints (3), (4), (7), (11), and (12). However, since $J$ is nonlinear in the binary matrices $\mathbf{X}$ and $\mathbf{Y}$, direct optimization of $J$ is cumbersome. We will therefore formulate an equivalent optimization problem which is simpler to solve. To this end, let us define two auxiliary matrices $\mathbf{V} \in \mathbb{R}^{N \times N \times F \times T}$ and $\mathbf{W} \in \mathbb{R}^{N \times N}$, where, for all $i, j$,

$$V_{i,j,f,t} \in \{v \in \mathbb{R} : v \leq X_{i,f,t}, v \leq Y_{j,f,t}\}, \tag{15}$$

$$W_{i,j} \in \{w \in \mathbb{R} : w \leq 1, w \leq \sum_{t=1}^{T} \sum_{f=1}^{F} V_{i,j,f,t}\}. \tag{16}$$

Now, for any fixed $\mathbf{X}$, $\mathbf{Y}$, it follows from (15) that

$$V^{\star}_{i,j,f,t} = \max V_{i,j,f,t} = \min\{X_{i,f,t}, Y_{j,f,t}\} = X_{i,f,t} Y_{j,f,t}. \tag{17}$$

The last equality in the above equation follows from the fact that both $X_{i,f,t}$ and $Y_{j,f,t}$ are boolean. Moreover, it follows from (16) and (12) that if $V_{i,j,f,t} = V^{\star}_{i,j,f,t}$, then

$$\max W_{i,j} = \min\{1, \sum_{t=1}^{T} \sum_{f=1}^{F} V^{\star}_{i,j,f,t}\} = Z_{i,j}. \tag{18}$$

Hence, for any fixed $\mathbf{X}$, $\mathbf{Y}$, $\mathbf{P}$ we can compute $J(\mathbf{X}, \mathbf{Y}, \mathbf{P})$ as the optimal value of objective of

$$J(\mathbf{X}, \mathbf{Y}, \mathbf{P}) = \max_{\mathbf{V}, \mathbf{W}} \quad \sum_{i=1}^{N} \sum_{\substack{j=1 \\ j \neq i}}^{N} W_{i,j} \tag{19a}$$
$$\text{s.t.} \qquad (15), (16)$$

Putting everything together, we arrive at the optimization problem

$$\max_{\mathbf{P},\mathbf{X},\mathbf{Y},\mathbf{V},\mathbf{W}} \sum_{i=1}^{N}\sum_{\substack{j=1,\\ j\neq i}}^{N} W_{i,j} \tag{20a}$$

s.t.

$$\sum_{i=1}^{N} X_{i,f,t}P_{i,t}H_{i,j} - \gamma^{\mathrm{T}} \sum_{\substack{f'=1\\ f'\neq f}}^{F}\sum_{k=1}^{N} A_{f',f}X_{k,f',t}P_{k,t}H_{k,j}$$

$$\geq \gamma^{\mathrm{T}}\sigma^2 - \gamma^{\mathrm{T}}(NP^{\max}+\sigma^2)(1-Y_{j,f,t}) \quad \forall\, j,f,t \tag{20b}$$

$$W_{i,j} \leq \sum_{t=1}^{T}\sum_{f=1}^{F} V_{i,j,f,t} \qquad \forall\, i,j \tag{20c}$$

$$W_{i,j} \leq 1 \qquad \forall\, i,j \tag{20d}$$

$$V_{i,j,f,t} \leq X_{i,f,t} \qquad \forall\, i,j,f,t \tag{20e}$$

$$V_{i,j,f,t} \leq Y_{j,f,t} \qquad \forall\, i,j,f,t \tag{20f}$$

$$\sum_{i=1}^{N} X_{i,f,t} \leq 1 \qquad \forall\, f,\, t \tag{20g}$$

$$\sum_{f=1}^{F} X_{i,f,t} \leq 1 \qquad \forall\, i,\, t \tag{20h}$$

$$0 \leq P_{i,t} \leq P^{\max} \qquad \forall\, i,t \tag{20i}$$

$$\mathbf{X},\mathbf{Y} \in \{0,1\}^{N\times F\times T} \tag{20j}$$

$$\mathbf{P} \in \mathbb{R}^{N\times T} \tag{20k}$$

$$\mathbf{V} \in \mathbb{R}^{N\times N\times F\times T} \tag{20l}$$

$$\mathbf{W} \in \mathbb{R}^{N\times N} \tag{20m}$$

The above problem formulation allows for full-duplex communication. Of course, if the self-channel power gain $H_{j,j}$ is sufficiently large compared with the inter-VUE channel power gains $H_{i,j}$, $i \neq j$, then (20) provides a half-duplex solution for scheduling and power control, i.e., that a VUE cannot receive packets at any RB $(f',t)$ while transmitting on RB $(f,t)$. However, if the diagonal elements of $\mathbf{H}$ are very large compared to the off-diagonal elements, this can cause numerical issues while solving (20). For this reason, when a half-duplex solution is implied by $\mathbf{H}$ (or otherwise desired), it is better to explicitly enforce a half-duplex solution by adding the constraint

$$Y_{j,f,t} \leq 1 - X_{j,f',t} \qquad \forall j,f,f',t \tag{20n}$$

and replacing $H_{i,j}$ with $\tilde{H}_{i,j}$ in (20b), where

$$\tilde{H}_{i,j} = \begin{cases} H_{i,j}, & i \neq j \\ 0, & \text{otherwise} \end{cases} \tag{21}$$

Replacing $\mathbf{H}$ with $\tilde{\mathbf{H}}$ is done solely for numerical reasons, since (20n) is sufficient to force the solution to be half-duplex.

We see that the problem (20), in its full-duplex and half-duplex formulation, has linear objective and constraints except the constraint (20b), which is quadratic. We call such a problem a MIQCP problem. Moreover, as shown in Appendix B, the problem is nonconvex, which will require a sophisticated and complex solver [20]. We will therefore not try to solve (20) directly, but will use it to find near-optimal schedules for fixed transmit powers and near-optimal power allocation for fixed schedules in Section IV-C and V-A, respectively.

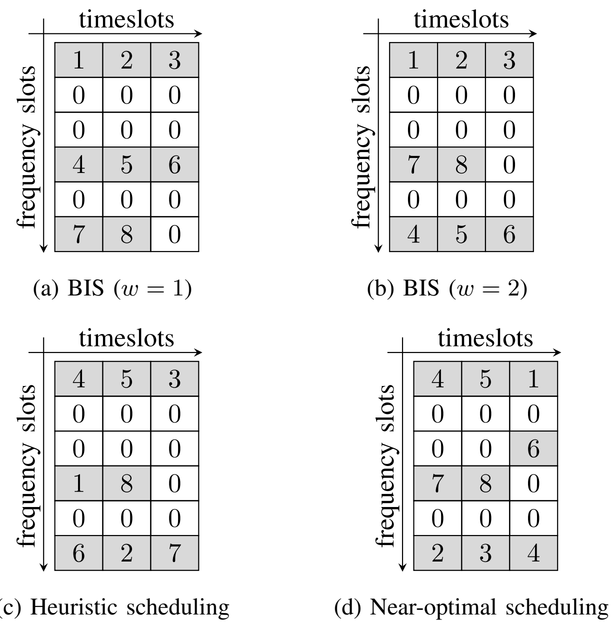


(a) BIS ($w = 1$)

(b) BIS ($w = 2$)

(c) Heuristic scheduling

(d) Near-optimal scheduling

Fig. 4: Example of VUE scheduling ($\mathbf{U}$) for $N = 8$, $F = 6$, and $T = 3$

## IV. Scheduling Algorithms

For the scheduling problem, without considering any power control, we set the transmit power for all VUEs to the maximum power $P^{\max}$, i.e., $P_{i,t} = P^{\max}\ \forall\, i,t$. For the sake of scheduling all available RBs, we define VUE 0 as a dummy VUE with zero transmit power. Hence, scheduling VUE 0 to an RB indicate that no VUE is scheduled in that RB.

Let us define the matrix $\mathbf{U} \in \{0,1,\ldots,N\}^{F\times T}$ to represent scheduled VUEs in an $F \times T$ RBs matrix. That is, $U_{f,t}$ is the VUE index scheduled in RB $(f,t)$. Fundamentally, scheduling is the process of allocating VUEs in available RBs, which is equivalent to populating the $\mathbf{U}$ matrix with appropriate VUE indices, as illustrated in Fig. 4. Once we have computed the matrix $\mathbf{U}$, we can compute $\mathbf{X}$ as follows,

$$X_{i,f,t} = \begin{cases} 1, & U_{f,t} = i \\ 0, & \text{otherwise} \end{cases} \tag{22}$$

### A. Block Interleaver Scheduler (BIS)

The approach here is to insert each VUE index exactly once in $\mathbf{U}$. Clearly, this is impossible if $N > FT$, i.e., when there are more VUEs than available RBs. For the time being, we will assume that $N \leq FT$ and treat the $N > FT$ case later in this Section. Moreover, we will assume that $N > T$, since

**Algorithm 1** Block Interleaver Scheduler (BIS)

**Input:** $\{N, F, T, w\}$
**Output:** $\mathbf{X}$

$\tilde{N} = \min\{\lfloor NT/2 \rfloor, N, FT\}$
$\tilde{F} = \lceil \tilde{N}/T \rceil$
Compute $\mathbf{f}$ and $\mathbf{n}$ from (23) and (25)
$\mathbf{f}' = \Pi(\mathbf{f}, w)$
$\mathbf{U} = \mathbf{0}^{F \times T}$
$k = 1$
**for** $l = 1 : |\mathbf{f}'|$ **do**
  $f' = f'_l$
  **for** $t = 1 : T$ **do**
    **if** $k \leq |\mathbf{n}|$ **then**
      $U_{f',t} = n_k$
      $k = k + 1$
    **end if**
  **end for**
**end for**
Compute $\mathbf{X}$ from $\mathbf{U}$ using (22)

the scheduling problem is otherwise trivial: we can simply schedule the VUEs in separate timeslots, which removes all ACI (and CCI) interference.

If $N > T$, then we need to multiplex VUEs in frequency, which results in ACI. To reduce the ACI problem, we strive to use as few frequency slots as possible and to space the frequency slots as far apart as possible. Since we can schedule $T$ VUEs per frequency slot, the smallest required number of frequency slots is $\tilde{F} = \lceil N/T \rceil$. Clearly, $\tilde{F} \leq F$, since we assume that $N \leq FT$. The selected frequency slots are put in the vector $\mathbf{f} \in \{1, 2, \ldots, F\}^{\tilde{F}}$. For BIS, we will use the frequency slots

$$f_k = 1 + \left\lceil (k-1)\frac{F-1}{\tilde{F}-1} \right\rfloor, \qquad k = 1, 2, \ldots, \tilde{F}. \tag{23}$$

We note that $f_1 = 1 < f_2 < \cdots < f_{\tilde{F}} = F$, and it can be shown that (23) maximizes the minimum distance between any two consecutive frequency slots, i.e., maximizes

$$\min_{l \in \{1,2,\ldots,\tilde{F}-1\}} |f_{l+1} - f_l|. \tag{24}$$

We initialize $\mathbf{U} = \mathbf{0}^{F \times T}$. Then, given $\mathbf{f}$, BIS starts by filling the rows of $\mathbf{U}$ in the natural way, i.e., row $f_1$ with VUE indices $1, 2, \ldots, T$, row $f_2$ with indices $T+1, T+2, \ldots, 2T$, and so on. To (possibly) improve the scheduler, the nonzero rows of $\mathbf{U}$ are then permuted with a block interleaver. In the actual implementation in Algorithm 1, we achieve the same result by first permuting $\mathbf{f}$ with the block interleaver $\Pi$ before filling in the rows of $\mathbf{U}$.

Now we explain the block interleaver $\Pi$ used to permute $\mathbf{f}$. Our block interleaver is similar to the one specified in 3GPP [16, section 5.1.4.2.1]. We define $\mathbf{f}' = \Pi(\mathbf{f}, w)$ as the output $\mathbf{f}'$ of a block interleaver with width $w \in \mathbb{N}$ and input vector $\mathbf{f}$. The block interleaver writes $\mathbf{f}$ row-wise in a matrix with width $w$, padding with zeros if necessary, then reads $\mathbf{f}'$ from the matrix column-wise ignoring zeros. Observe that if $w = 1$, then the block interleaver output is same as the input, i.e., $\mathbf{f}' = \mathbf{f}$. The width of the block interleaver is an input to this algorithm.

As an example, when $N = 8, F = 6, T = 3, w = 1$, we compute $\mathbf{f}' = \mathbf{f} = [1, 4, 6]$, and schedule VUEs accordingly as shown in Fig. 4 (a). Similarly, Fig. 4 (b) shows the result when $w = 2$ and the computed $\mathbf{f}' = [1, 6, 4]$. We present the results for various values of block interleaver widths in Section VI-B.

Now let us treat the case when $N > FT$. One way to handle this case is to schedule only $\tilde{N} \leq FT$ of the $N$ VUEs. For BIS, we put the selected VUEs in the vector $\mathbf{n} \in \{1, 2, \ldots, N\}^{\tilde{N}}$, where

$$n_k = 1 + \left\lceil (k-1)\frac{N-1}{\tilde{N}-1} \right\rfloor, \qquad k = 1, 2, \ldots, \tilde{N}. \tag{25}$$

We note that if $\tilde{N} = N$, then $\mathbf{n} = [1, 2, \ldots, N]$. Hence, the two cases $N \leq FT$ and $N > FT$ can be unified by letting $\tilde{N} = \min\{N, FT\}$ and $\tilde{F} = \lceil \tilde{N}/T \rceil$.

However, if $T = 1$, then it is never advantageous to schedule more than $\lfloor N/2 \rfloor$ VUEs in the half-duplex case. To understand why, we note that since we have $\tilde{N}$ transmitters and $N - \tilde{N}$ receivers, the maximum number of successful links we can ever hope for is $\tilde{N}(N - \tilde{N}) = (N/2)^2 - (\tilde{N} - N/2)^2$, which is maximized by selecting $\tilde{N}$ as large as possible, but still less or equal to $\lfloor N/2 \rfloor$, i.e., $\tilde{N} = \min\{\lfloor N/2 \rfloor, F\}$. Scheduling more than $\lfloor N/2 \rfloor$ VUEs will not increase the number of possible links (due to half-duplex transmission), but increase ACI (due to more transmitters), which can never be beneficial. The final, unifying, calculation of $\tilde{N}$ in Algorithm 1 is therefore $\tilde{N} = \min\{\lfloor TN/2 \rfloor, N, FT\}$ and $\tilde{F} = \lceil \tilde{N}/T \rceil$, which covers all cases of $N$, $F$, and $T$.

### B. Heuristic Scheduling Algorithm

The approach taken here is to loop through all RBs and schedule either a real or dummy VUE to each RB. The scheduling decision is taken in a greedy fashion. That is, we strive to schedule the best possible VUE to the RB under the assumption that the schedule for all previous RBs is fixed. The resulting schedule can schedule a VUE, zero, one, or multiple times, as opposed to BIS, which schedules all real VUEs exactly once (if there are enough RBs, $FT \geq N$ and $T > 1$).

The heuristic algorithm is executed in two steps. In the first step, we determine the RB scheduling order, and in the second step, we use this order to visit the RBs and schedule VUEs sequentially.

Now we explain the first step, i.e., the procedure to compute the scheduling order $\mathbf{f}$ for frequency slots. We note that $\mathbf{f}$ is a permutation of $\{1, 2, \ldots, F\}$, and we can therefore choose $\mathbf{f}$ in $F!$ possible ways. We compute $\mathbf{f}$ using a greedy algorithm as shown in Algorithm 2.1. While constructing $\mathbf{f}$, our priority is to spread out the consecutive scheduling frequency slots in order to minimize the received ACI. Therefore, in each iteration, we are scheduling a frequency slot with minimum

**Algorithm 2.1** Computation of scheduling order $\mathbf{f}$

**Input:** $\{F, \mathbf{A}\}$
**Output:** $\mathbf{f}$

1: $f_1 = 1$
2: $\mathcal{F} = \{2, 3, \dots, F\}$
3: **for** $l = 2 : F$ **do**
4: $\quad \mathcal{G} = \operatorname*{argmin}_{f \in \mathcal{F}} \sum_{l'=1}^{l-1} A_{f_{l'}, f}$
5: $\quad f_l = \max \left\{ \operatorname*{arg\,max}_{f \in \mathcal{G}} \sum_{l'=1}^{l-1} |f - f_{l'}| \right\}$
6: $\quad \mathcal{F} = \mathcal{F} \setminus f_l$
7: **end for**

**Algorithm 2.2** Heuristic Scheduling Algorithm

**Input:** $\{N, F, T, \mathbf{H}, \mathbf{A}, \mathbf{P}, \gamma^{\mathrm{T}}, \sigma^2\}$
**Output:** $\mathbf{X}$

$\mathbf{X} = \mathbf{0}^{N \times F \times T}, \quad \mathbf{U} = \mathbf{0}^{F \times T}$
Compute $\mathbf{f}$ using Algorithm 2.1
// Schedule RBs in the order specified by $\mathbf{f}$
**for** $l = 1 : F$ **do**
$\quad f = f_l$
$\quad$ **for** $t = 1 : T$ **do**
$\quad\quad$ // Schedule VUE in RB $(f, t)$
$\quad\quad$ **for** $i = 0 : N$ **do**
$\quad\quad\quad U_{f,t} = i$
$\quad\quad\quad$ Compute $\mathbf{X}$ from $\mathbf{U}$ using (22)
$\quad\quad\quad$ Compute $\mathbf{Z}$ for $\mathbf{X}$ using (12)
$\quad\quad\quad s_i = \sum_{m=1}^{N} \sum_{\substack{j=1,\\ j \neq m}}^{N} Z_{m,j}$
$\quad\quad$ **end for**
$\quad\quad U_{f,t} = \arg\max_i \{s_i\}$
$\quad$ **end for**
**end for**
Compute $\mathbf{X}$ from $\mathbf{U}$ using (22)

received ACI from all the scheduled frequency slots. Therefore, we always start scheduling from the first frequency slot, i.e., $f_1 = 1$, then we find out the next frequency slot $f_2$ as the unscheduled frequency slot with minimum received ACI from $f_1$. We repeat this process until all frequency slots are chosen. Finding the frequency slot with minimum received ACI from all the scheduled frequency slots is actually not possible, since we do not know yet which VUE is going to be scheduled in the RBs. Therefore, we compute the ACI in an unscheduled frequency slot by assuming unit transmit power and unit channel gain from all interferers. If there are multiple unscheduled frequency slots with the same minimum affected ACI, then we choose the frequency slot having maximum average distance from all the scheduled frequency slots. If there is still a tie, then we pick the maximum out of it as shown in Algorithm 2.1, line 5. This way, we ensure that $f_2 = F$ for a typical ACIR model.

Next we explain the second step, i.e., finding out the VUE to schedule in an RB. The algorithm is stated in Algorithm 2.2. Given an RB to schedule, first we compute the total number of successful links upon scheduling each VUE in the chosen RB, and then we pick the VUE which would maximize this quantity. Observe that VUE 0 (the dummy VUE) can be scheduled to the RB, which, of course, means that no real VUE is scheduled.

The result of the scheduling when $N = 8, F = 6, T = 3$, is shown in Fig. 4 (c), when VUEs are placed on a one lane road, with equal distances $d_{\text{avg}}$ (refer to Table II) to the neighboring VUEs, and by assuming zero shadow loss. Note that in this example VUE 4 is scheduled twice.

### C. Near-Optimal Scheduling

Observe that, if we fix $\mathbf{P}$, e.g., $P_{i,t} = P^{\max}\ \forall i, t$, then the MIQCP optimization problem (20) translates into a BLP problem. We compute a near-optimal scheduling by solving this BLP problem formulation using the Gurobi solver [21], which internally uses the branch and bound method. However, due to the computational complexity of the problem, branch and bound method involves a number of linear optimizations which, in the worst case, is believed to be exponential in the number of binary variables. Since finding an optimal solution would be time consuming, we stop the simulation when the solver attains a 5% optimality gap, i.e., when the attained objective value is no less than 95% of the optimum objective value. An example of the near-optimal scheduling is given in Fig. 4 (d), when VUEs are placed on a one lane road, with equal distance $d_{\text{avg}}$ to the neighboring VUEs and by assuming zero shadow loss.

## V. Power Control Algorithms

### A. Near-Optimal Power Control

Observe that for the scheduling algorithms in Section IV, we fixed $\mathbf{P}$, thereby converting the nonconvex MIQCP problem in (20) into a BLP problem. Similarly, once we find out a scheduling matrix $\mathbf{X}$, we can convert (20) into a power-control problem by inputting $\mathbf{X}$ and making $\mathbf{P}$ as an optimization variable. The resulting problem is an MILP problem. In summary, the optimal power values can be computed by solving (20), with the following modified objective function,

$$\max_{\mathbf{P}, \mathbf{Y}, \mathbf{V}, \mathbf{W}} \sum_{i=1}^{N} \sum_{\substack{j=1,\\ j \neq i}}^{N} W_{i,j} - \beta \sum_{t=1}^{T} \sum_{i=1}^{N} P_{i,t}, \tag{26}$$

Note that $\beta$ is the weight of the total power consumption in the objective, in order to achieve our secondary goal of minimizing the total power consumption. The value of $\beta$ is set to a small value $1/(NTP^{\max})$, so that the sum power will not affect our major goal of maximizing the total number of successful links.

Observe that the problem of finding the optimal power values is NP-hard as proved in [15, Lemma 1]. We use Gurobi [21] to solve the above power control problem. Since finding the optimal solution is very time consuming, we stop the solver when it attains a 5% optimality gap, like we do in the near-optimal scheduling

### B. Heuristic Power Control

Since the exponentially increasing worst-case complexity of optimal power control is problematic in practice for large networks, we propose a heuristic power control algorithm which has polynomial time computational complexity. The proposed heuristic power control algorithm is an extension of our previous work on power control [15] and the work of Kang Wang et al. [22]. All those previous works assumes $T = 1$, whereas our proposed algorithm finds a power control solution for any value of $T$. The algorithm is described in Algorithm 3.

The SINR $\Upsilon_{i,j,t}$ of a link $(i,j)$ during the timeslot $t$ is computed as follows,

$$\Upsilon_{i,j,t} = \frac{\sum\limits_{f=1}^{F} X_{i,f,t} P_{i,t} H_{i,j}}{\sigma^2 + \sum\limits_{f=1}^{F} \sum\limits_{f'=1}^{F} \sum\limits_{\substack{k=1 \\ k \neq i}}^{N} X_{i,f,t} A_{f',f} X_{k,f',t} P_{k,t} H_{k,j}}. \quad (27)$$

The derivation of the above equation is explained in Appendix A. A link $(i,j)$ is successful if and only if its SINR is greater than or equal to $\gamma^{\mathrm{T}}$ on any timeslot, i.e., $\Upsilon_{i,j,t} \geq \gamma^{\mathrm{T}}$ for any $t \in \{1, 2, \ldots, T\}$. Our goal is to find the optimal transmit power value for each VUE in each timeslot in order to maximize the total number of successful links. The algorithm is an iterative algorithm involving two steps in each iteration. Since it may not be possible to ensure success for all links, our first step is to find the set of candidate links $\mathcal{L}$. The second step is to compute the power values $P_{i,t}$ for all VUEs in all timeslots in order to maximize the number of successful links in $\mathcal{L}$. Therefore, we update both $\mathcal{L}$ and $P_{i,t}\ \forall i,t$ on each iteration. We terminate the algorithm, when we observe that all the links in $\mathcal{L}$ are achieving the SINR target $\gamma^{\mathrm{T}}$.

Now we explain the first step, i.e., the computation of $\mathcal{L}$ on each iteration. In the first iteration, we initialize $\mathcal{L}$ to the set of all links, and in subsequent iterations we remove some of the links from $\mathcal{L}$, thereby making $\mathcal{L}$ a nonincreasing set over iterations. We initialize all VUEs transmit power to $P^{\text{init}}$, i.e., $P_{i,t} = P^{\text{init}}\,\forall i,t$. We then define the variable $\tilde{P}_{i,j,t}$ as the required transmit power of VUE $i$ during the timeslot $t$ in an iteration, so that the link $(i,j)$ would be successful in the next iteration, under the assumption that the interference remains constant. The value of $\tilde{P}_{i,j,t}$ is computed in each iteration as shown in Algorithm 3, line 8. If the required power for a link $(i,j)$ is more than $P^{\max}$, i.e., $\tilde{P}_{i,j,t} > P^{\max}\,\forall t$, then the link $(i,j)$ is declared as a broken link. The set of broken links $\mathcal{B}$ in an iteration is computed in Algorithm 3, line 9. We find out repeatedly broken links over many iterations and remove them from the set $\mathcal{L}$.

In order to find the repeatedly broken links, a counter $C_{i,j}$ is set to count the number of iterations at which the link $(i,j)$ gets broken. We remove the link $(i,j)$ from $\mathcal{L}$ once $C_{i,j}$ reaches above a threshold $C^{\mathrm{T}}$, i.e, $C_{i,j} > C^{\mathrm{T}}$. We observe that, the algorithm shows improved performance as we increase $C^{\mathrm{T}}$. However, higher values of $C^{\mathrm{T}}$ result in

**Algorithm 3** Heuristic Power Control

**Input:** $\{N, F, T, P^{\text{init}}, P^{\max}, \mathbf{X}, \mathbf{H}, \mathbf{A}, \gamma^{\mathrm{T}}, \sigma^2\}$
**Output:** $\mathbf{P}$

1: $P_{i,t} = P^{\text{init}} \quad \forall i,t$
2: $\mathbf{C} = \mathbf{0}^{N \times N}$
3: $\mathcal{L} = \{(i,j) : \sum\limits_{t=1}^{T} \sum\limits_{f=1}^{F} X_{i,f,t} > 0, j \neq i\}$ // set of candidate links
4: $\mathcal{T}_i = \{t : \sum\limits_{f=1}^{F} X_{i,f,t} > 0\} \quad \forall i$ // scheduled timeslots for VUE $i$
5: Compute SINR $\Upsilon_{i,j,t} \quad \forall i,j,t$ using (27)
6: **while** $\exists\,(i,j) \in \mathcal{L}$ s.t. $\Upsilon_{i,j,t} < \gamma^{\mathrm{T}} \quad \forall t$ **do**
7: // Compute the required power and broken links $\mathcal{B}$
8: $\tilde{P}_{i,j,t} = \frac{\gamma^{\mathrm{T}}}{\Upsilon_{i,j,t}} P_{i,t} \quad \forall (i,j) \in \mathcal{L}, t \in \mathcal{T}_i$
9: $\mathcal{B} = \{(i,j) : \tilde{P}_{i,j,t} > P^{\max} \quad \forall t \in \mathcal{T}_i\}$
10: // Increment $C_{i,j}$ and update $\mathcal{L}$
11: $C_{i,j} = C_{i,j} + 1 \quad \forall (i,j) \in \mathcal{B}$
12: $\mathcal{L} = \mathcal{L} \setminus \{(i,j) : C_{i,j} > C^{\mathrm{T}}\}$
13: $\mathcal{R}_i = \{j : (i,j) \in \mathcal{L} \setminus \mathcal{B}\} \quad \forall i$
14: // Compute power values
15: $P_{i,t} = 0 \ \ \forall i,t$
16: **for** $i = 1 : N$ **do**
17: **while** $\mathcal{R}_i \neq \emptyset$ **do**
18: $\mathcal{K}_t = \{\tilde{P}_{i,j,t} : \tilde{P}_{i,j,t} \leq P^{\max},\ j \in \mathcal{R}_i\}\ \forall t \in \mathcal{T}_i$
19: $t^{\star} = \mathrm{rand}(\arg\max\limits_{t \in \mathcal{T}_i} |\mathcal{K}_t|)$
20: $P_{i,t^{\star}} = \max \mathcal{K}_{t^{\star}}$
21: $\mathcal{R}_i^{\star} = \{j : P_{i,t^{\star}} \geq \tilde{P}_{i,j,t^{\star}}\}$
22: $\mathcal{R}_i = \mathcal{R}_i \setminus \mathcal{R}_i^{\star}$
23: **end while**
24: $\mathcal{T}_i = \mathcal{T}_i \setminus \{t : P_{i,t} = 0\}$
25: **end for**
26: Compute SINR $\Upsilon_{i,j,t}\ \forall i,j,t$ using (27) with updated power values
27: **end while**

more number of iterations, thereby increasing computational complexity. Moreover, we note that the initial transmit power $P^{\text{init}}$ plays a crucial role in this algorithm. A higher value of $P^{\text{init}}$ leads to more number of broken links in the first iteration itself, whereas lower values lead to a slow convergence of the algorithm. By simulations, we observe that $P^{\text{init}} = P^{\max}/10$ is a reasonable value for $P^{\text{init}}$.

Next we explain the second step, i.e., the computation of power values $P_{i,t}\ \forall t$, in each iteration. We compute the power values of each VUE independently. In the following, we therefore explain the power value computation of an arbitrary VUE $i$ for all timeslots $t \in \{1, 2, \ldots, T\}$. Let us define the set $\mathcal{R}_i$ as the set of intended receivers in $\mathcal{L} \setminus \mathcal{B}$ when the transmitter is VUE $i$, as computed in Algorithm 3, line 13. Our goal is to make the received SINR of all the links from VUE $i$ to VUEs in $\mathcal{R}_i$ equal to or greater than $\gamma^{\mathrm{T}}$ in the next iteration, i.e., $\Upsilon_{i,j,t} \geq \gamma^{\mathrm{T}} \ \forall j \in \mathcal{R}_i$ . Therefore, we compute $P_{i,t} \ \forall t$, such that the SINR values of all the links in $\mathcal{L} \setminus \mathcal{B}$ are greater or equal to $\gamma^{\mathrm{T}}$ on at least one of the timeslots in the next iteration, under the assumption that the interference remains constant.

Furthermore, in order to minimize the interference to other links, we would consider allocating power to a VUE in as few number of timeslots as possible. Therefore, the power allocation to VUE $i$ involves two steps. The first step is to decide the optimal timeslot $t^\star$ to allocate power, and the second step is to compute the power value for the chosen timeslot $t^\star$. We compute $t^\star$ as the timeslot at which VUE $i$ can serve the maximum number of intended receivers in $\mathcal{R}_i$. For this purpose, we first formed $\mathcal{K}_t$ as the set of transmit powers for VUE $i$ that are required to serve the receivers in $\mathcal{R}_i$ and do not exceed $P^{\max}$, as shown in Algorithm 3, line 18. We note that the cardinality of this set, i.e., $|\mathcal{K}_t|$, is the number of receivers that can be served during timeslot $t$ in the next iteration. Therefore, we compute $t^\star$ as the timeslot $t$ that maximizes $|\mathcal{K}_t|$. If there are multiple timeslots with the same maximum number of receivers, then we randomly pick one among them using $\mathrm{rand}$ function. We define $s = \mathrm{rand}(\mathcal{S})$ as an element randomly chosen with uniform probability from the set $\mathcal{S}$. Then we compute the power value $P_{i,t^\star}$ as the maximum value in $\mathcal{K}_{t^\star}$ (which is less than $P^{\max}$), as shown in Algorithm 3, line 20. Then we compute the set of receivers $\mathcal{R}_i^\star$ which are served by the allocated power $P_{i,t^\star}$, and remove those from $\mathcal{R}_i$. Therefore, the set $\mathcal{R}_i$ remains as the set of VUEs not yet served. We repeat these two steps until the allocated transmit power $P_{i,t}$ is greater or equal to the required transmit power $\tilde{P}_{i,j,t}$ on at least one of the timeslot $t$, for all receivers in $\mathcal{R}_i$.

The algorithm is convergent as proved in Lemma 1 in Appendix C. However, in order to ensure a fast convergence and improved performance, we restrict allocating power values to VUE $i$ only in a limited number of timeslots $\mathcal{T}_i$. In each iteration, we compute the set $\mathcal{T}_i \ \forall i$, as the set of timeslots during which VUE $i$ is allocated with nonzero power values. In the subsequent iterations, we allocate power values to VUE $i$ only in those timeslots specified by $\mathcal{T}_i$.

## VI. Performance Evaluation

### A. Scenario and Parameters

We consider a network consisting of $N$ VUEs distributed on a one-lane road, and each VUE tries to broadcast a message to all other VUEs. The distance between any two adjacent VUEs, $d$, follows a shifted exponential distribution, with the minimum distance $d_{\min}$ and the average distance $d_{\text{avg}}$. That is, the probability density function of $d$ is given as,

$$f(d) = \begin{cases} (1/(d_{\text{avg}} - d_{\min}))\exp(-\frac{d-d_{\min}}{d_{\text{avg}}-d_{\min}}), & d \geq d_{\min} \\ 0, & \text{otherwise} \end{cases} \tag{28}$$

We choose $d_{\text{avg}} = 48.6\,\text{m}$ for a vehicular speed of $70\,\text{km/h}$, as recommended by 3GPP [23, section A.1.2] for freeway scenario. However, we did not adopt the channel model Winner+B1 used by 3GPP evaluation scenario [23], since it is not appropriate for highway scenarios. Instead, we adopted the channel model from [24], which is a model based on the measurements of V2V links at carrier frequency 5.2 GHz in a highway scenario. The path loss in dB for a distance $d$ is computed as,

$$\mathrm{PL}(d) = \mathrm{PL}_0 + 10n\log_{10}(d/d_0) + X_{\sigma_1} \tag{29}$$

where $n$ is the path loss exponent, $\mathrm{PL}_0$ is the path loss at a reference distance $d_0$, and $X_{\sigma_1}$ represents the shadowing effect modeled as a zero-mean Gaussian random variable with standard deviation $\sigma_1$. The values of the channel parameters are taken from [24] and shown in Table II. An additional attenuation of $10\,\text{dB}$ is added as penetration loss for each obstructing VUE [25]. The noise variance is $-95.2\,\text{dBm}$ and $P^{\max}$ is $24\,\text{dBm}$ as per 3GPP recommendations [18]. We assume that $d_{\min} = 10\,\text{m}$ and that $\gamma^{\mathrm{T}} = 5\,\text{dB}$ is sufficient for a transmission to be declared as successful (i.e., that the error probability averaged over the small-scale fading is sufficiently small). Additionally, we fix $C^{\mathrm{T}} = 100$, which is found to be a reasonable value for the heuristic power control algorithm.

TABLE II: System Simulation Parameters

| Parameter | Value |
|---|---|
| ACIR model | 3GPP mask |
| $\gamma^{\mathrm{T}}$ | 5 dB |
| $P^{\max}$ | 24 dBm |
| $P^{\text{init}}$ | $P^{\max}/10$ |
| $\mathrm{PL}_0$ | 63.3 dB |
| $n$ | 1.77 |
| $d_0$ | 10 m |
| $\sigma_1$ | 3.1 dB |
| Penetration Loss | 10 dB per obstructing VUE |
| $\sigma^2$ | $-95.2$ dBm |
| $d_{\text{avg}}$ | 48.6 m |
| $d_{\min}$ | 10 m |
| $\beta$ | $1/(NP^{\max})$ |
| $\eta$ | $\gamma^{\mathrm{T}}(NP^{\max} + \sigma^2)$ |
| $C^{\mathrm{T}}$ | 100 |

### B. Simulation Results

To measure the performance, we use the average number of successful links per VUE, defined as,

$$\bar{Z} = \frac{1}{N}\sum_{i=1}^{N}\sum_{\substack{j=1\\ j\neq i}}^{N} \mathrm{E}[Z_{i,j}], \tag{30}$$

where the expectation is taken over the random quantities in the experiment, i.e., the inter-VUE distances and shadow fading. The metric $\bar{Z}$ can be interpreted as the average number of VUEs that can decode a packet from a certain VUE. Clearly, we would like to ensure that $\bar{Z}$ is sufficiently large to support the application in mind. However, to specify this minimum acceptable value of $\bar{Z}$ is out of scope of this paper.

Since the block interleaver width $w$ is an input parameter to BIS, we considered a class of BIS with all possible $w \in \{1, 2, \ldots, \tilde{F}-1\}$. We present here the results for the optimal $w$ which maximizes $\bar{Z}$ under the assumption of equal transmit powers, shown as the blue curves marked with triangles in

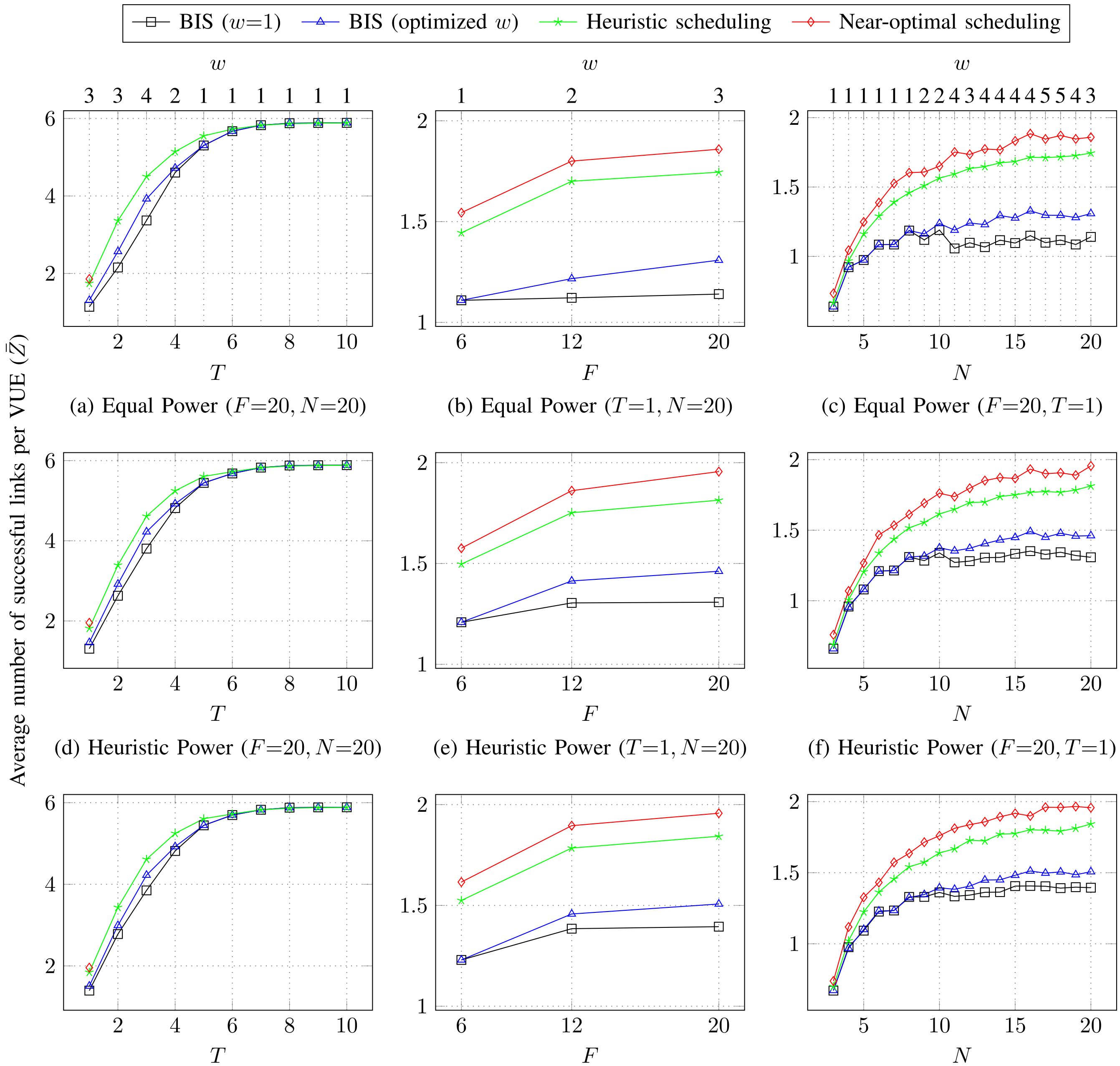


(a) Equal Power ($F$=20, $N$=20)

(b) Equal Power ($T$=1, $N$=20)

(c) Equal Power ($F$=20, $T$=1)

(d) Heuristic Power ($F$=20, $N$=20)

(e) Heuristic Power ($T$=1, $N$=20)

(f) Heuristic Power ($F$=20, $T$=1)

(g) Near-optimal power ($F$=20, $N$=20)

(h) Near-optimal power ($T$=1, $N$=20)

(i) Near-optimal power ($F$=20, $T$=1)

Fig. 5: Average number of successful links per VUE ($\bar{Z}$) for various scheduling algorithms

Fig. 5. The corresponding $w$ for BIS is shown as an extra x label on top of Fig. 5(a)–(c), and we do not vary $w$ with respect to the power control algorithms.

In Fig. 5, we present the result for various values of $F$, $T$, $N$, and various scheduling and power control algorithms. However, we have not simulated near-optimal scheduling for $T > 1$, due to its very high computational complexity.

In Fig. 5(a), we plot $\bar{Z}$ by varying $T$ for a fixed $F$ and $N$. The results in Fig. 5(a) clearly show that $\bar{Z}$ is severely limited by ACI when many VUEs must be multiplexed in frequency, i.e., when $T$ is small compared to $N$. This motivates the search for scheduling and power control methods to mitigate the ACI problem in this situation. We also observe that $\bar{Z}$ remains essentially constant for $T \geq 10$.

One way to limit the effect of ACI would be to increase $F$ (for a fixed $N$ and $T$) to allow for larger spacing of VUEs in frequency. However, the results in Fig. 5(b) show that $\bar{Z}$ is only slowly increasing with $F$. On the other hand, Fig. 5(b) shows that significant gains can be achieved by more advanced scheduling than using a BIS.

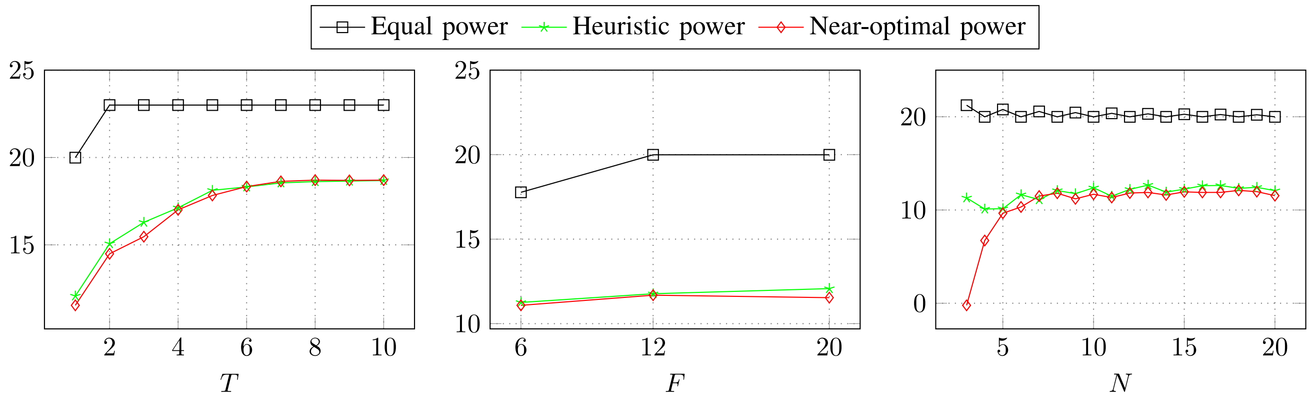


(a) ($F$=20, $N$=20) (b) ($T$=1, $N$=20) (c) ($F$=20, $T$=1)

Fig. 6: Average transmit power per VUE (dBm) for various power control algorithms for BIS ($w$=1)

Moreover, for a fixed $T$ and $F$, we see in Fig. 5(c) that $\bar{Z}$ is increasing with $N$, at least for the more advanced schedulers. This might be surprising at first sight; however, this effect is not unreasonable, since more receivers become available for each transmission when $N$ increases. In other words, the number of terms in the double sum in (30) increases, which tends to increase $\bar{Z}$. The results in Fig. 5(c) also show that significant gains can be achieved with proper scheduling.

As seen in Fig. 5(d)–(i), power control increases performance, but, in general, the gains are marginal for advanced schedulers. The performance gain is more significant for the BIS scheduler compared to the more advanced schedulers. This can be explained by the fact that a suboptimal schedule can be corrected to some degree by power control. Indeed, assigning zero or a very low power to a VUE effectively changes the schedule for that VUE. For instance, that the performance for BIS with $w = 1$ for large $N$ is significantly improved with power control, as seen in Fig. 5(f) and Fig. 5(i).

In Fig. 6, we plot the average transmitter power values for various power control algorithms, upon fixing the scheduling algorithm as BIS with $w = 1$. We observe that our proposed heuristic power control algorithm uses less transmit power compared to equal power, and close to the transmit power used by near-optimal power control.

The simulation results presented here is for half-duplex communication scenario, i.e., a VUE cannot receive any packets in any frequency slots while transmitting in a timeslot. For detailed results on full-duplex communication, interested readers are directed to our report in the archive [19]. Moreover, in [19] we present similar results for both full-duplex and half-duplex scenarios, with both SCFDMA and 3GPP mask ACIR models. We observe that the near-optimal scheduling algorithm show significant performance improvement for full-duplex communication scenarios when ACIR equals to 3GPP mask. We also plot the average transmit power values for various scheduling algorithms in [19], and observe the similar trends for various scheduling algorithms. Additionally, the MATLAB code used for the simulation is shared on github [26].

## VII. Conclusion

This paper studies performance of V2V all-to-all broadcast communication in a one-lane highway scenario where co-channel interference is removed by not allowing more than one transmitting VUE per time-frequency resource block. From the results presented in this paper, which are for half-duplex communication, we can draw the following conclusions.

1) Performance is mainly limited by ACI when VUEs are multiplexed in frequency.
2) Performance is heavily dependent on scheduling and power allocation.
3) In general, scheduling with fixed and equal transmit powers is more effective in improving performance than subsequent power control.
4) To find a schedule and power allocation to maximize performance can be stated as the nonconvex mixed integer quadratic constrained programming (MIQCP) problem in (20).
5) To find a schedule to maximize performance for a fixed power allocation can be stated as a Boolean linear programming (BLP) problem found by fixing $\mathbf{P}$ to a constant matrix in (20).
6) The heuristic scheduling algorithm for a fixed power allocation defined in Algorithm 2.2 has significantly lower complexity than the BLP program and performs significantly better than the baseline block-interleaver scheduler defined in Algorithm 1.
7) To find a power allocation to maximize performance for a fixed schedule can be stated as the mixed integer linear programming (MILP) problem found by replacing the objective in (20) with (25) and fixing $\mathbf{X}$.
8) The heuristic power allocation algorithm for a fixed schedule defined in Algorithm 3 achieve similar performance as the solution to the MILP problem, but at a significantly lower computational complexity.
9) For small problems, the tandem of Algorithms 2.2 and 3 perform close to the near-optimum solution obtained by

solving, in sequence, the BLP and MILP problems in items 5) and 7) above, respectively.

## Appendix A
## Joint Scheduling and Power Control Problem Formulation by Focusing on Transmitter-Receiver Links

Let us define $\mathbf{\Upsilon} \in \mathbb{R}^{N\times N\times T}$ with $\Upsilon_{i,j,t}$ being the SINR during timeslot $t$ for the link from VUE $i$ to VUE $j$, i.e., transmitter-receiver link $(i,j)$. The value of $\Upsilon_{i,j,t}$ can be computed as follows,

$$\Upsilon_{i,j,t} = \frac{\sum_{f=1}^{F} X_{i,f,t}P_{i,t}H_{i,j}}{\sigma^2 + \sum_{f=1}^{F}\sum_{f'=1}^{F}\sum_{\substack{k=1\\k\neq i}}^{N} X_{i,f,t}A_{f',f}X_{k,f',t}P_{k,t}H_{k,j}} \tag{31}$$

where $\sigma^2$ is the noise variance and $P_{i,t}$ is the transmit power of VUE $i$ during timeslot $t$.

Now we explain each component of (31). Observe that $X_{i,f,t}P_{i,t}H_{i,j}$ in numerator is the received signal power for the link $(i,j)$ on RB $(f,t)$, therefore, $\sum_f X_{i,f,t}P_{i,t}H_{i,j}$ is the total received signal power in timeslot $t$. Similarly $A_{f',f}X_{k,f',t}P_{k,t}H_{k,j}$ is the interference power received by VUE $j$ on RB $(f,t)$ from VUE $k$ when VUE $k$ is scheduled to transmit on RB $(f',t)$. Similarly, $X_{i,f,t}A_{f',f}X_{k,f',t}P_{k,t}H_{k,j}$ is the same received interference power if VUE $i$ is scheduled to transmit in RB $(f,t)$. Therefore, $\sum_f\sum_{f'}\sum_{k\neq i} X_{i,f,t}A_{f',f}X_{k,f',t}P_{k,t}H_{k,j}$ is the total interference power received to the link $(i,j)$ if VUE $i$ is scheduled to transmit in any of the RBs in timeslot $t$.

However, translating the constraint for achieving SINR target, i.e., $\Upsilon_{i,j,t} \geq \gamma^{\mathrm{T}}$, we get the following constraint,

$$\begin{aligned}&\sum_{f=1}^{F} X_{i,f,t}P_{i,t}H_{i,j}\\ &\quad -\gamma^{\mathrm{T}}\sum_{f=1}^{F}\sum_{f'=1}^{F}\sum_{\substack{k=1\\k\neq i}}^{N} X_{i,f,t}A_{f',f}X_{k,f',t}P_{k,t}H_{k,j} \geq \gamma^{\mathrm{T}}\sigma^2\end{aligned} \tag{32}$$

Observe that the above constraint is more complicated than a quadratic constraint. Moreover, we can simplify the above constraint only upto a boolean quadratic constraint for a scheduling problem, upon fixing the power values $P_{i,t}\,\forall\, i,t$.

## Appendix B
## Proving the Nonconvexity of (20b)

Let us represent (20b) as follows,

$$G(\mathbf{P},\mathbf{X},\mathbf{Y}) \leq 0 \tag{33}$$

where $G(\mathbf{P},\mathbf{X},\mathbf{Y})$ is defined as follows,

$$\begin{aligned}G(\mathbf{P},\mathbf{X},\mathbf{Y}) = &\\ -\sum_{i=1}^{N} X_{i,f,t}P_{i,t}H_{i,j} &+ \gamma^{\mathrm{T}}\sum_{\substack{f'=1\\f'\neq f}}^{F}\sum_{k=1}^{N} A_{f',f}X_{k,f',t}P_{k,t}H_{k,j}\\ &+\gamma^{\mathrm{T}}\sigma^2 - \gamma^{\mathrm{T}}(NP^{\max}+\sigma^2)(1-Y_{j,f,t})\end{aligned} \tag{34}$$

We prove the nonconvexity of (20b) by proving that $G(\mathbf{P},\mathbf{X},\mathbf{Y})$ is nonconvex. We prove this by proving that the Hessian matrix of $G(\mathbf{P},\mathbf{X},\mathbf{Y})$ is not positive semidefinite, with respect to the two variables $x = X_{1,f,t}$ and $y = P_{1,t}$. The Hessian matrix of $G(\mathbf{P},\mathbf{X},\mathbf{Y})$ with respect to $x$ and $y$ is as follows,

$$\nabla^2 G = \begin{bmatrix}\frac{\partial^2 G}{\partial^2 x} & \frac{\partial^2 G}{\partial y\partial x}\\ \frac{\partial^2 G}{\partial x\partial y} & \frac{\partial^2 G}{\partial^2 y}\end{bmatrix} \tag{35}$$

However, observe that $\frac{\partial^2 G}{\partial^2 x} = \frac{\partial^2 G}{\partial^2 y} = 0$, and $\frac{\partial^2 G}{\partial x\partial y} = \frac{\partial^2 G}{\partial y\partial x}$ from (34). Therefore, the determinant of the above Hessian matrix is $\left|\nabla^2 G\right| = -(\frac{\partial^2 G}{\partial x\partial y})^2 \leq 0$. Since $\frac{\partial^2 G}{\partial x\partial y} \neq 0$ for some $j,f,t$, the corresponding determinant of the Hessian matrix is negative. Hence the function $G(\mathbf{P},\mathbf{X},\mathbf{Y})$ is nonconvex. This concludes the proof.

## Appendix C
## Proving the Convergence of Algorithm 3

*Lemma 1:* The Algorithm 3 is convergent.

*Proof:* Observe that the set $\mathcal{L}$ is nonincreasing on each iteration. When the termination condition (Algorithm 3, line 6) is not satisfied, the set of broken links $\mathcal{B}$ is nonempty. This implies that, the counter $C_{i,j}$ is incremented for some $(i,j) \in \mathcal{L}$ in each iteration. Therefore, the maximum number of iterations possible before the set $\mathcal{L}$ becomes empty is $C^{\mathrm{T}}\,|\mathcal{L}|$. This concludes the proof. ■

## References


[1] W. Sun, E. G. Ström, F. Brännström, K. C. Sou, and Y. Sui, “Radio resource management for D2D-based V2V communication,” *IEEE Transactions on Vehicular Technology*, vol. 65, no. 8, pp. 6636–6650, Aug 2016.

[2] L. Gallo and J. Härri, “Short paper: A LTE-direct broadcast mechanism for periodic vehicular safety communications,” in *IEEE Vehicular Networking Conference*, Boston, USA, Dec. 2013, pp. 166–169.

[3] W. L. Tan, K. Bialkowski, and M. Portmann, “Evaluating adjacent channel interference in IEEE 802.11 networks,” in *Proc. IEEE Vehicular Technology Conference*, Taipei, Taiwan, May 2010.

[4] E. Dahlman, S. Parkvall, and J. Sköld, “4G: LTE/LTE-Advanced for mobile broadband.” Oxford: Academic Press, 2011, pp. 370–371.

[5] W. Li, X. Ma, J. Wu, K. S. Trivedi, X. L. Huang, and Q. Liu, “Analytical model and performance evaluation of long-term evolution for vehicle safety services,” *IEEE Transactions on Vehicular Technology*, vol. 66, no. 3, pp. 1926–1939, March 2017.

[6] J. Zhou, R. Q. Hu, and Y. Qian, “Message scheduling and delivery with vehicular communication network infrastructure,” in *2013 IEEE Global Communications Conference (GLOBECOM)*, Atlanta, USA, Dec 2013, pp. 575–580.

[7] F. Zeng, R. Zhang, X. Cheng, and L. Yang, “Channel prediction based scheduling for data dissemination in VANETs,” *IEEE Communications Letters*, vol. 21, no. 6, pp. 1409–1412, 2017.

[8] W. Li, J. Chen, H. Long, and B. Wu, “Performance and analysis on LTE system under adjacent channel interference of broadcasting system,” in *2012 IEEE 12th International Conference on Computer and Information Technology*, Chengdu, China, Oct 2012, pp. 290–294.

[9] Q. Wang and X. Li, “Analysis of LTE FDD and TD-LTE combination network’s interference,” in *2016 2nd IEEE International Conference on Computer and Communications (ICCC)*, Chengdu, China, Oct 2016, pp. 2332–2336.

[10] J. Ribadeneira-Ramirez, G. Martinez, D. Gomez-Barquero, and N. Cardona, “Interference analysis between digital terrestrial television (DTT) and 4G LTE mobile networks in the digital dividend bands,” *IEEE Transactions on Broadcasting*, vol. 62, no. 1, pp. 24–34, March 2016.

[11] "CEPT Report 40: Compatibility study for LTE and WiMAX operating within the bands 880-915 MHz / 925-960 MHz and 1710-1785 MHz / 1805-1880 MHz (900/1800 MHz bands)," Tech. Rep., CEPT Electronic Commun. Committee (ECC), Nov 2010.

[12] L. Wang, X. Qi, and K. Wu, "Embracing adjacent channel interference in next generation wi-fi networks," in *2016 IEEE International Conference on Communications (ICC)*, Kuala Lumpur, Malaysia, May 2016.

[13] A. Adya, P. Bahl, J. Padhye, A. Wolman, and L. Zhou, "A multi-radio unification protocol for IEEE 802.11 wireless networks," in *First International Conference on Broadband Networks*, San Jose, CA, USA, Oct 2004, pp. 344–354.

[14] J. Nachtigall, A. Zubow, and J. P. Redlich, "The impact of adjacent channel interference in multi-radio systems using IEEE 802.11," in *2008 International Wireless Communications and Mobile Computing Conference*, Crete Island, Greece, Aug 2008, pp. 874–881.

[15] A. Hisham, W. Sun, E. G. Ström, and F. Brännström, "Power control for broadcast V2V communications with adjacent carrier interference effects," in *IEEE International Conference on Communications (ICC)*, Kuala Lumpur, Malaysia, May 2016.

[16] 3GPP, "Evolved Universal Terrestrial Radio Access (E-UTRA); Physical channels and modulation," 3rd Generation Partnership Project (3GPP), TR 36.211, March 2017. [Online]. Available: http://www.3gpp.org/ftp/Specs/archive/36_series/36.211

[17] T. Svensson and T. Eriksson, "On power amplifier efficiency with modulated signals," in *Proc. IEEE Vehicular Technology Conference*, Ottawa, Canada, May 2010.

[18] 3GPP, "Evolved Universal Terrestrial Radio Access (E-UTRA); Radio Frequency (RF) system scenarios," 3rd Generation Partnership Project (3GPP), TR 36.942, Oct. 2014. [Online]. Available: http://www.3gpp.org/ftp/Specs/html-info/36942.htm

[19] "Additional Results of Scheduling and Power Control for Broadcast V2V Communications with Adjacent Channel Interference," Tech. Rep., Aug. 2017. [Online]. Available: https://arxiv.org/src/1708.02444/anc/Additional_Results.pdf

[20] Y. Nesterov, "Semidefinite relaxation and nonconvex quadratic optimization," *Optimization Methods and Software*, vol. 9, no. 1-3, pp. 141–160, 1998.

[21] Gurobi Optimization, Inc., "Gurobi optimizer reference manual," 2015. [Online]. Available: http://www.gurobi.com

[22] K. Wang, C. Chiasserini, J. Proakis, and R. Rao, "Joint scheduling and power control for multicasting in wireless ad hoc networks," in *Proc. IEEE Vehicular Technology Conference*, vol. 5, Florida, USA, Oct. 2003, pp. 2915–2920.

[23] 3GPP, "Technical Specification Group Radio Access Network; Study on LTE-based V2X Services," 3rd Generation Partnership Project (3GPP), TR 36.885, June 2016. [Online]. Available: http://www.3gpp.org/ftp/Specs/html-info/36885.htm

[24] J. Karedal, N. Czink, A. Paier, F. Tufvesson, and A. Molisch, "Path loss modeling for vehicle-to-vehicle communications," *IEEE Transactions on Vehicular Technology*, vol. 60, no. 1, pp. 323–328, Jan. 2011.

[25] D. Vlastaras, T. Abbas, M. Nilsson, R. Whiton, M. Olbäck, and F. Tufvesson, "Impact of a truck as an obstacle on vehicle-to-vehicle communications in rural and highway scenarios," in *Proc. IEEE 6th International Symposium on Wireless Vehicular Communications*, Vancouver, Canada, 2014.

[26] *Matlab code for V2V communication*, Aug. 2017. [Online]. Available: https://github.com/anverhisham/Scheduling_and_powerControl_in_V2V_Communication